Joint range assignment and routing to conserve energy in wireless ad hoc networks

Sajjad Zarifzadeh [a],[*], Amir Nayyeri [b], Nasser Yazdani [a], Ahmad Khonsari [a], Hamid Hajabdolali Bazzaz [a]

[a] The Router Laboratory, ECE Department, University of Tehran, Tehran, Iran
[b] The Computer Science Department, University of Illinois at Urbana-Champaign, IL, United States

ARTICLE INFO

ABSTRACT

In wireless ad hoc networks, energy utilization is perhaps the most important issue, since it corresponds directly to the operational network lifetime. Topology Control (TC) is a well-known energy saving technique which tries to assign transmission ranges of nodes to optimize their energy utilization while keeping the network connected. In current TC schemes, the transmission range of each node is mostly accounted as the exclusive estimator for its energy consumption, while ignoring the amount of data it forwards. Especially when such schemes are coupled with the popular shortest path routing, they usually create a highly-loaded area at the center of the network in which nodes deplete their battery very quickly. In this paper, we introduce efficient strategies that take both load and range into account to handle this problem. We first consider the *simple strategy* in which a proper transmission range is computed for all nodes of the network to optimize their energy utilization under the presence of the shortest path routing. Inspiring from the results of this strategy, we then propose our *combined strategy* and argue that a combination of circular paths and shortest paths could result in a much better solution. We also provide detailed analytical models to measure the forwarding load and interference of nodes and then corroborate them with simulation results. Using the combined strategy, the achieved improvement in terms of traffic load, interference, and maximum energy consumption is about 50%, as compared with the simple strategy.

1. Introduction

Wireless ad hoc networks consist of resource-constrained wireless devices which can communicate with each other in the absence of any specific infrastructure. Energy conservation is one of the most important concerns in ad hoc networks, since battery replacement or power recharging is usually difficult. This issue becomes even more vital in some special-purposed ad hoc networks, such as wireless sensor networks (WSN) where nodes are deployed in disastrous or military environments.

Thus far, various techniques have been suggested to optimize the network's energy consumption at different layers of the network protocol stack [1], ranging from efficient hardware design [2], to efficient placing of communicating codes in the network [3]. *Topology control* (TC), as one of the most well-known solutions for this problem, is based on construction of an efficient network topology for the network in which the energy consumption is optimized while essential properties of the topology such as connectivity are preserved [4]. One of the simplest, yet realistic, TC problems (known as *Range Assignment* problem) is "how to find a minimum transmission range for each network node so that the topology remains

* Corresponding author. Tel.: +98 21 61114352.
  E-mail addresses: szarifzadeh@ece.ut.ac.ir (S. Zarifzadeh), nayyeri2@uiuc.edu (A. Nayyeri), yazdani@ut.ac.ir (N. Yazdani), ak@ipm.ir (A. Khonsari), h.hajabdolali@ece.ut.ac.ir (H.H. Bazzaz).

connected" [5]. The main intuition behind the range assignment problem is the fact that amount of communication energy that each node consumes is highly proportional to its transmission range. Hence, as much as we reduce the range of nodes, their power is expected to drain more slowly.

However, we believe there is a shortcoming in most of the existing TC approaches; as a matter of fact, current solutions often neglect the impact of traffic load on the energy utilization of nodes. For instance, in the existing conventional range assignment problem, the goal of optimization is solely about minimizing the transmission range of wireless devices, while in practice both the range and the traffic load of each device determine its energy consumption rate. Particularly, the problem appears more acute when the shortest path (SP) routing method is used to establish multihop communications between nodes [6]. In this situation, it is observed that nodes near the center of the network have to forward data for a large number of other nodes. As a consequence, these centric nodes deplete their energy much faster than peripheral ones, which may eventually result in the early partitioning of network topology.

In brief, the intention of this paper is to overcome the aforementioned deficiency by taking both traffic load and transmission range of nodes into account when optimizing nodes' energy utilization. In particular, we define a new problem, called *Single-range Energy Conservation* (*SEC*) problem, whose objective is finding a single transmission range for all nodes to minimize their maximum energy utilization. After presenting a general description for this problem, we introduce two separate strategies to solve it. First, we explain the *simple strategy* in which the routing method is fixed to the well-known shortest path routing. Besides, we present separate analytical models to capture characteristics of nodes with respect to the traffic load and interference parameters. The results of these models clearly indicate that this strategy fails to distribute the load appropriately among nodes and still creates a hot spot region at the center of the network. Inspiring from these results, we then propose the *combined strategy* to further elongate network lifetime. The basic idea is to use the redundant energy capacity of peripheral nodes to reduce the load of hot spots, by using a proper combination of shortest paths and circular paths. For each strategy, we present an analytical method to calculate the optimal values of configuration parameters, like transmission range. In fact, the true purpose of our mathematical models is to find the optimal configuration point of each strategy for any given network setting, without running simulation. Finally, we perform simulations to validate our modeling and also to compare the results of different strategies with each other.

The rest of the paper is organized as follows: in the next section, we review the previous works on energy conserving techniques in wireless ad hoc networks. In Section 3, we present the motivation behind our work, the exact description of the assumed network model and the SEC problem. Section 4 analyzes the problem for the simple strategy where the shortest path method is applied to route traffic. Section 5 is devoted to the explanation of our combined strategy. Simulation results are provided in Section 6 and finally, we conclude the paper in Section 7.

2. Related work

Thus far, different techniques have been proposed to reduce the amount of energy required for communications between nodes in wireless ad hoc networks. A challenging relevant problem is how to choose the transmission range (or the transmission power) of wireless nodes in a way that their energy utilization is minimized, while some essential properties, like connectivity, are preserved in the resulted network. In [4], the authors provide a general formulation for this problem (known as *Topology Control* problem) along with some efficient algorithms to solve it. In their graph-based model, this problem is represented by a triple $\langle M, P, O \rangle$ where M is the corresponding model of the graph, i.e., directed or undirected, P represents the network properties that are important to preserve, such as connectivity or strong connectivity, and finally O denotes the optimization objective like the maximum or the total power consumption. Categorizing different versions of the topology control problem according to this model, they present valuable results, including polynomial algorithms for some and proof of NP-hardness for others.

In addition, there are many other works that consider the problem from a more practical perspective. As one of the initial papers, [7] suggests two centralized algorithms along with two heuristic distributed methods. In addition, Wattenhofer et al. in [8] propose an elegant distributed algorithm which works locally. The idea is to adjust transmission range of every node such that it has at least one neighbor on each α angle. Surprisingly, they proved that the global connectivity will be conserved if α is not bigger than $2\pi/3$. Another worth noting work is [5], in which the authors attempt to find an equal and small range value for all nodes to get a strongly connected graph structure. They apply a probabilistic method rather than deterministic algorithms (as the typical approach in other proposals) to attain such property.

Other practical approaches are COMPOW [9] and CLUSTERPOW [10], which are implemented in the network layer. Both of these works rely on the idea that if each node uses the smallest common power required to maintain connectivity, then the capacity of the entire network with respect to carrying traffic is maximized, the battery life is extended, and the MAC-level contention is mitigated. The major drawback of these two approaches is their significant message overhead, since each node has to run multiple daemons, each of which should exchange state information with their counterparts at other nodes. In [11], the authors propose an efficient topology control algorithm that adjusts nodes' power, such that all nodes together form a topology which is energy efficient simultaneously for both unicast and broadcast communications.

One of the challenging issues in realizing topology control protocols is reducing the computational and message overhead of running such protocols in such a way that they can react to the topological changes in the network quickly and efficiently. In response to this issue, recently

several algorithms have been introduced which construct the topology in a localized manner [12–14]. The localized topology control technique lets each wireless node adjust its transmission power using only the local information (i.e., the topological information of nodes within a constant number of intermediate hops), while it maintains a decent global structure to support energy efficient communication. In addition, several algorithms have been suggested that try to form a simple unit disk graph[1] between nodes to minimize their energy consumption [15–18]. Most of these works try to find either analytically or experimentally a single minimum transmission range for all nodes, called *Critical Transmission Range*, such that there is at least one path between every pair of nodes in the resulted topology.

Moreover, a number of routing protocols have been proposed to establish multihop communication in ad hoc networks [19–22]. Traditionally, these protocols are evaluated in terms of packet loss ratio, routing message overhead, and route length [23,24]. However, since wireless networks are often composed of battery-powered devices, energy consumption is also an important metric [24]. So far, there have been several works for energy efficient routing in wireless ad hoc and sensor networks, such as [25,26]. Five important metrics for energy efficient routing are studied in [26], like minimizing energy consumed per packet, minimizing variance in node power levels, minimizing cost per packet, and so on. As the choice of topology can greatly influence the performance of the employed routing method, some works have considered both topology control and routing simultaneously to provide energy efficient communication in ad hoc networks [27,28].

One fundamental shortcoming which has appeared in almost all of these proposals is that they neglect the impact of traffic load on the energy utilization rate of nodes. However, as we will show in this work, energy consumption in each wireless device is considerably affected by the volume of traffic it relays. As a result, often some negative phenomena happen in the process of data forwarding in ad hoc networks. For example, one negative phenomenon which is frequently observed in such environments is the appearance of a highly-loaded and early-depleted area in the centric part of the network [6,30]. This deficiency is emerged, since in hop-by-hop communications usually most of packets should pass over this small area on their way to the destinations.

3. Motivation and modeling

Energy consumption in wireless ad hoc networks is usually traced to either communication or processing efforts of the system. However, in many cases like sensor networks, the amount of energy that nodes use for message passing is an order of magnitude higher than what they consume for processing. Thus, in many proposals in this field, optimizing the communication's energy consumption is considered as the ultimate objective.

3.1. Basics of wireless communication

Communication's energy consumption is itself caused by either transmitting or receiving packets. Here, we have used the well-known modeling, also used by Jones et al. [1] and Pan et al. [29]. In this model, the required energy for transmitting a bit-stream at rate r over the Euclidian distance of l is assessed by

$$E_t(r, l) = r(\gamma + \alpha l^n), \tag{1}$$

where γ is the distance-independent term (i.e., the energy utilized in the transmitter circuit) and α captures the distance-dependent one [29]. Moreover, n is a real value which is often $2 \leqslant n \leqslant 4$ for the free-space and short-to-medium range communication. Likewise, the amount of energy required to receive a bit-stream again at rate r is

$$E_{rec}(r) = r\beta, \tag{2}$$

where β is a constant value. Since $E_t \gg E_{rec}$ [1], we here restrict our attention to that portion of energy used for transmitting data. Therefore, when a node sends data by rate r over distance l, it consumes $E(r,l)$ units of energy per time where $E(r,l)$ is computed according to the following formula:

$$E(r, l) = E_t(r, l) = r(\gamma + \alpha l^n). \tag{3}$$

3.2. Motivation

The above relation apparently shows that the amount of energy consumed in a wireless device not only depends on its transmission range but also on the volume of the traffic it relays. In other words, if all nodes have roughly the same range, nodes with a higher forwarding load lose their energy much faster than those which forward a limited number of packets. Consequently, it seems quite rational to exploit the energy capacity of lightly-loaded nodes to reduce the energy consumption of hot spots. Unfortunately, due to the dual role[2] of transmission range in energy utilization function, handling this problem is not straightforward.

Indeed, the intention of this paper is to prolong the network lifetime[3] through an efficient combination of both range assignment and load balancing approaches. Notice that while managing the topology in this manner can result in a longer network lifetime, it may increase the total energy consumption of nodes. Yet, most of works in this field try to increase the lifetime of the network rather than its total energy consumption [7]. One simple reason is that when a wireless network gets partitioned, the amount of energy remained in the still alive nodes may be not of much importance.

---

[1] An undirected graph in which there is a link between any pair of nodes whose distance is smaller than unit (or a fixed value r).

[2] According to (3), the selection of smaller ranges seems to reduce the consumed energy. But, it may eventually worsen the story, because the forwarding load increases drastically as ranges get very small.

[3] In this context, the network lifetime is the time elapses from the network start-up time till the first node of the network stops working. So, the goal is to maximize the minimum lifetime value in the set of all nodes.

3.3. Network model and problem statement

Our network model is very similar to the ones used in [6,30]. We assume an ad hoc network which consists of a set of wireless nodes that are uniformly distributed with density δ within a circle C_{OR} of center O and radius R. Each node sends messages to any other node with an average uniform rate λ per flow. The transmission range of all nodes is the same and also configurable to a real value T. An arbitrary node A can directly communicate with any other node within the distance of its transmission range. The transmission range T along with the geographical positions of nodes in the network represents the topology as an undirected graph in which there is a link between any pair of nodes which can communicate directly. Since both node distribution and traffic rate are uniform, the traffic model used in this paper is supposed to be symmetric in the sense that all nodes of the same distance from the center are similar. In other words, the forwarding load of nodes, which are of an equal distance from the center, is the same.

Now, let us define some important concepts before specifying our problem. The *load* of node A is the average rate of traffic that A either sends or relays. We use $L(d)$ to denote the load of a node placed at distance d from the center O. $L(d)$, itself, is composed of two major parts: (i) *Sending load* $L_s(d)$ (i.e., the load on the node due to sending its own traffic), and (ii) *Forwarding load* $L_f(d)$, (i.e., the load on the node due to forwarding traffic of other nodes). Based on this network model, we have

$$L_s(d) = (\pi R^2 \delta - 1)\lambda \approx \pi R^2 \delta \lambda. \tag{4}$$

However, as we will show later, the computation of $L_f(d)$ is not an easy task; in fact, it requires some sort of modeling about the characteristics of routing paths in the network. We also use $E(d)$ to refer to the average rate of energy consumed by a node at distance d from the center. Based on (3), we can compute $E(d)$ by

$$E(d) = L(d) \cdot (\gamma + \alpha T^n), \tag{5}$$

where T is the value of the transmission range. We call all nodes inside the transmission disk[4] of a node A as the *coverage set* of A. The *interference of a node* A is defined as the number of paths that go through at least one node in the coverage set of A. The intuition behind this definition is that when node A sends data, it definitely collides with all the traffic flows passing over the nodes in the coverage set of A. According to our uniform traffic rate assumption, it is expected that the node of maximum interference yields the maximum actual interference in practice too, even though its real occurrence depends on the actual traffic pattern of flows.

We define the notion of *network lifetime* as the time interval from the network deployment till the first node failure in the network [31,32]. In order to elucidate the relationship between energy utilization and network lifetime, we provide our definition of energy efficiency: A protocol is called *energy efficient*, if it minimizes the maximum

energy consumption of nodes for fulfilling its task. The objective of minimizing the maximum energy utilization rather than the total over all nodes is because battery life is a local resource so the collective minimization has a little practical value [1]. Assuming that all nodes have the same initial power, it is not difficult to understand that an energy efficient protocol necessarily maximizes the network lifetime too. Hence, our problem of maximizing the network lifetime converts to the following min–max problem, called *Single-range Energy Conservation* (*SEC*) problem:

> **Given**: A wireless network field deployed within C_{OR}, with node density δ, an average traffic rate λ between every pair of nodes, and a certain routing strategy.
> **Optimization goal**: Minimize $\max\{E(d)|0 < d < R\}$.
> **Variables**: Transmission range T, and routing parameters of the given strategy.
> **Constraints**: Routing constraints of the given strategy.

It is worth mentioning that most of the existing approaches, when specifying the problem and devising a solution, do not take either transmission range or routing constraints into account. In this paper, we aim to show how a joint consideration of the range assignment and routing algorithms can yield a much better solution.

4. The simple strategy

In this section, we study the SEC problem in the simple strategy where the method of routing is fixed to the typical shortest path (SP) routing. We first analyze the distribution of load and interference in this strategy and then present mathematical relations to obtain the optimal transmission range.

4.1. Load distribution analysis

In [30], Pham and Perreau introduce a simple model (known as *rectangle model*) for determining the load distribution on ad hoc networks that use single-path routing. In [6], the authors extend this model to the case of multipath routing. In both works, the analysis shows that the load gets maximized at the center of the network and as a result, when all nodes are of the same power, nodes at the center form a bottleneck that affects the throughput of the whole system. However, these models do not pay any attention to the transmission range, while this factor seems to significantly impact the amount of forwarding load on nodes. Below, we introduce a new model for finding the load distribution of nodes in a network that uses the SP routing. To simplify our modeling, we here assume an ideal load balanced SP routing protocol; we refer the reader to [33] for a profile of such protocols. These protocols can greatly help to balance the load, while preserving the SP paradigm in principle.

Let T be the value of the transmission range chosen for all network nodes. In order to provide strong connectivity between nodes, there should be a lower bound on T. This lower bound (referred to by *Critical Transmission Range* or T_{min}) is mainly governed by the node density

---

[4] Transmission disk of a node v is a disk centered at v with a radius equal to the transmission range of v.
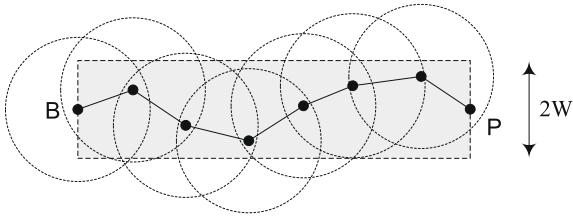
Fig. 1. The rectangle model.

δ and can be estimated through analytical methods or experiments [15–18]. Now, consider two nodes B and P in the network. If the network is relatively dense, the shortest path between these two nodes will be very close to the line segment connecting two nodes together [6,30]. However, we can generally expect that the routing path lies inside a rectangle, formed between B and P, whose length is the same as the distance between B and P and its width is $2W$, as depicted in Fig. 1. In the case that the SP routing is used, the average value of W (which is used to model all routes) is determined by the node density δ and the network radius R, and is supposed to be independent of T^5 [6]. It is remarkable that, since W is related to δ, the rectangle model remains valid even for the case of sparse networks; namely, a wider rectangle is used for a network with a lower density. As this model is just like the one proposed by Ganjali and Keshavarzian [6] to model paths in multipath routing, we first sketch their analytical modeling.

Let A and P be two fixed points (or two nodes) inside C_{OR} and d_{AP} denote the geographical distance between these nodes. Also, assume that P is the center of an infinitesimal area that measures $dx \times dy$. According to the above discussion, the set of nodes used by a routing path between any two nodes lies inside a rectangle of width $2W$. Ganjali and Keshavarzian suggest that if $d_{AP} > W$, the locus of a node B whose path towards P goes through A, should meet two constraints: (1) the distance from point A to the line segment BP should be less than W, and (2) the projection of point A on BP should lie between B and P. The locus of B which is derived from these two constraints is illustrated by the area S_2 in Fig. 2a. On the other hand, they conclude that, when $d_{AP} \leqslant W$, the locus of B is the intersection of C_{OR} with a half plane whose boundary goes over A and is perpendicular with AP. This section is demonstrated by the combination of S_1 and S_2 in Fig. 2b.

Intuitively, the average forwarding load on node A for transferring traffic towards node P is proportional to S_2/S_1. The intuition is that all the traffic from nodes inside S_2 towards P should pass over nodes of S_1. Since we have assumed a load balanced routing, this load would be

shared among the nodes in S_1; therefore, the load on node A which is produced by forwarding traffic of S_2 towards P is proportional to S_2/S_1. Following the model introduced in [6], it is also reasonable to assume that nodes within distance T of P share the load of the whole traffic sent from nodes inside the shaded segment in Fig. 2b (i.e., the area S_1 and S_2). To compute the total traffic which pass through A, we are to consider all different positions of point P, and sum up the load on A, for each possible position of P. However, calculation of the load distribution in this manner results in a very complex integral, which can only be computed through numerical methods and hence can not provide us enough insight into the system performance. Instead, through extending the approach used in [34] to compute the load of nodes in a sensor network, we could simplify the model to get a closed form expression for $L_f(d)$.

Consider the area S_3 which is a sector centered around AP with an angle θ (Fig. 3). Now, let us assume a new model where node A which is at distance d from O has the duty of forwarding the traffic from nodes in S_3 towards P. Clearly, this model is equivalent to the previous one, if $|S_2| = |S_3|$ (we use $|S|$ to refer to the area of S). Given two points A and P, since $|S_2|$ decreases with increasing d_{AP} (if $d_{AP} > W$), then both $|S_3|$ and θ are decreasing functions of d_{AP}. If we can find a sector $\bar{S}_3$ with angle $\bar{\theta}$ that is equivalent to S_2 on average and is decoupled from d_{AP}, our estimation (i.e., $|S_2| = |S_3|$) would be justified for every position of A and P.

Obviously, finding a value of $\bar{\theta}$ that satisfies $|S_2| = |S_3|$ on average for every pair of points A and P is very difficult. However, it is observed that the area S_3 is mostly dependent on its height, i.e., d_{AD}, rather than θ, because $|S_3| \approx d_{AD}^2 \theta / 2$. Hence, we can compute $\bar{\theta}$ when A is placed at the center and then apply this value as an estimation for every node A. In Appendix I, we use this simplification to estimate $\bar{\theta}$. As an instance, we get $\bar{\theta} = 0.7$ for the case that $\delta = 2$ and $R = 10$. Moreover, Appendix I presents a way to get a closed form expression for calculation of $L_f(d)$. In brief, we have

$$L_f(d) \approx \frac{(R^2 - d^2)^2}{T^2} \bar{\theta} \delta \lambda. \tag{6}$$

4.2. Interference distribution analysis

In Section 3, we introduced our definition of interference as the number of paths which go through at least one node in the coverage set of node. Clearly, to compute the interference, we should know the exact position of all nodes in the network and this unfortunately makes our modeling untractable. Instead, we here define a weaker definition which is much easier to compute, while estimating the original interference well. Formally, a path *intersects* with a disk, if at least one of its links crosses (or lies inside) the circumference of the disk. We define the *virtual interference of a node A* as the number of all paths intersecting with the transmission disk of A. It is not difficult to realize from this definition that as much as the virtual interference of a node becomes higher, the likelihood of the actual interference caused by

---

[5] Our simulation results confirm that the average value of W is independent of T, unless T is so large that most of nodes can communicate directly to each other. The approach we use in this paper to determine the value of W (with respect to a specific density and radius) is its approximation through averaging among all the paths in the sample graph formed with the critical transmission range T_{min}. For example, we get $W = 1$ for the case that $\delta = 2$ and $R = 10$.
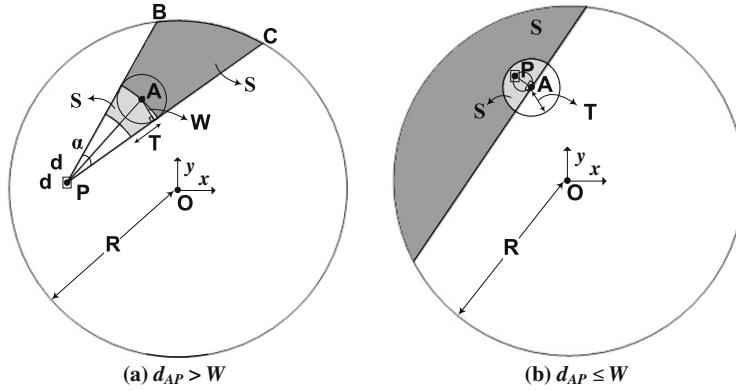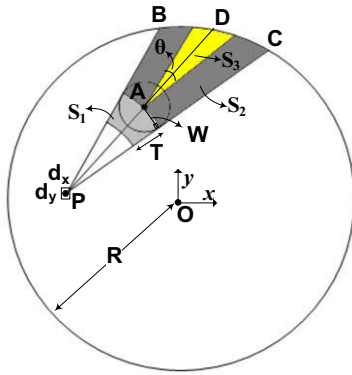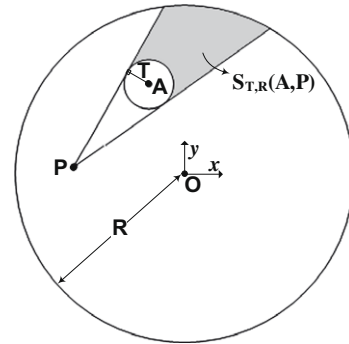
Fig. 2. Load distribution in the simple strategy.

Fig. 3. Approximating the area S_2 by the area S_3.

Fig. 4. The area of $S_{T,R}(A,P)$.

this node increases, as well. However, unlike the original interference, the virtual interference of a node can be estimated without the need to know which nodes are exactly in its coverage set. This is due to the fact that by replacing coverage set with transmission disk in the new definition, we can apply geometric methods to approximate the number of paths that intersect with the disk. Let $VI(d)$ be the amount of virtual interference of a node placed at distance d from the center. Now, we show how to measure $VI(d)$ based on the characteristics of paths in the simple strategy. But, before continuation of the paper, we should describe an elementary definition which is frequently referred to in the rest of the paper. Consider two fixed points A and P where point A is within C_{OR} while P can be everywhere. As shown in Fig. 4, we define $S_{T,R}(A,P)$ as the area which is formed between two circles C_{OR} and C_{AT}[6] and surrounded by two tangent lines drawn from P to the circle C_{AT}. To compute $S_{T,R}(A,P)$, a mathematical method similar to the one introduced in [6] can be used.

Again, assume that A is a point at distance d from the center and P is a fixed point inside C_{OR}. We want to find the set of all points B such that the shortest path between P and B intersects with the transmission disk of A. In order

to compute the locus of point B, we have to consider two separate cases:

(i) if $d_{AP} > T$, then point B should satisfy two constraints: (1) the distance from A to the line segment PB should be less than T, and (2) the projection of point A on line PB should lie between P and B. The above two constraints lead us to the area $S_{T,R}(A,P)$ and C_{AT} as the locus of all points B, which is illustrated by the grayed area in Fig. 5a. Notice that for the sake of simplicity, we here ignore the impact of W on the virtual interference of nodes.

(ii) if $d_{AP} \leqslant T$, then the locus of all points B is the area of the whole network region C_{OR} (Fig. 5b). This is because every path towards P intersects with the transmission disk of A.

Let $VI(A,P)$ be the area of the region which is the locus of point B, as described above in cases (i) and (ii). It is apparent that if we multiply $VI(A,P)$ by the node density δ, then we get the number of nodes that have the property that their paths towards P potentially intersect with the transmission disk of A. Thus, to compute the total virtual interference of A, we need to consider all possible positions of point P, and sum up $\delta \cdot VI(A,P)$ for each position of P. Considering (x,y) as the coordinates of point P, we can mathematically express $VI(d)$ as

---

[6] C_{AT} is a circle with radius T centered at point A
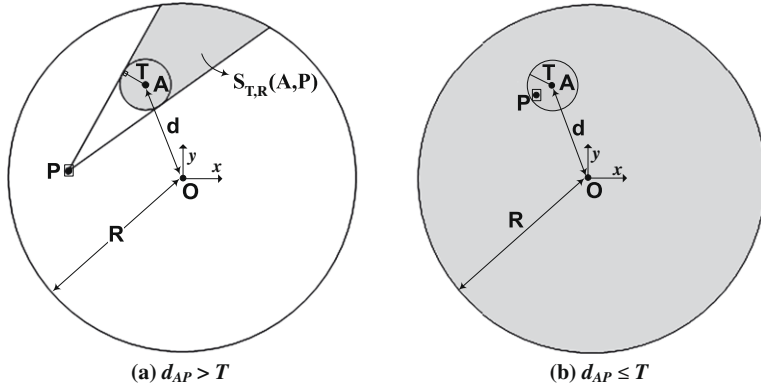
(a) $d_{AP} > T$ (b) $d_{AP} \leq T$

Fig. 5. Virtual interference distribution in the simple strategy.

$$VI(d) = \int \int_{\forall P \in C_{OR}} \delta \cdot VI(A,P)\delta \, dx \, dy$$
$$= \int \int_{\forall P \in C_{OR} - C_{AT}} \delta \cdot (S_{T,R}(A,P) + \pi T^2)\delta \, dx \, dy$$
$$+ \delta \pi R^2 \times \delta \pi T^2, \tag{7}$$

where the first and the second term in above sum formulize $VI(A,P)$ for the cases (i) and (ii), respectively. In some communication environments, the interference range of wireless devices turns out to be larger than their transmission range. In this case, the interference range should be replaced by T in (7).

4.3. Calculating the optimal transmission range

Now, we show how to find the optimal range value for all nodes of the network to minimize the maximum energy consumption among them and then analyze the solution with respect to the forwarding load and interference parameters.

From (6), we can immediately conclude that as much as a node is nearer to the center (i.e., d is smaller), it will have a higher rate of forwarding load. Combining (4)–(6), we get

$$E(d) = (L_f(d) + L_s(d)) \cdot (\gamma + \alpha T^n)$$
$$\approx \delta\lambda\left(\frac{(R^2 - d^2)^2}{T^2}\bar{\theta} + \pi R^2\right) \cdot (\gamma + \alpha T^n). \tag{8}$$

Since all nodes have the same transmission range, we can infer that similar to the forwarding load, the energy consumption rate reaches its pick at the center of the field, where $d = 0$. This maximum energy is

$$E(0) \approx \delta\lambda\left(\frac{R^4}{T^2}\bar{\theta} + \pi R^2\right) \cdot (\gamma + \alpha T^n)$$
$$= \delta\lambda R^2\left(\frac{R^2}{T^2}\bar{\theta} + \pi\right) \cdot (\gamma + \alpha T^n). \tag{9}$$

Our goal is to find the optimal T that minimizes $E(0)$. Taking derivative from $E(0)$ with respect to T and setting it to zero, the following equation is obtained (after some simplifications) where its root determines the best value of T:

$$n\pi\alpha T^{n+2} + (n - 2)R^2\bar{\theta}\alpha T^n - 2R^2\bar{\theta}\gamma = 0. \tag{10}$$

Fig. 6 demonstrates the analytical results of $E(0)$ with respect to T in a network with $\delta = 2$, $R = 10$, $W = 1$, $\bar{\theta} = 0.7$, $\alpha = 1$, $\gamma = 1$, $\lambda = 1$, and n = 3. The minimum
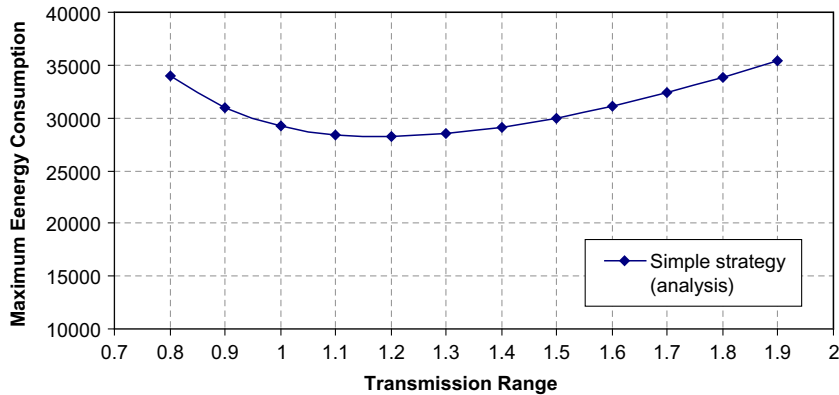

Fig. 6. Analytical results of the maximum energy utilization in the simple strategy under different values of transmission range T.

value of $E(0)$ is achieved at $T \approx 1.2$. Interestingly, as we can see from the diagram, minimizing T does not necessarily reduce the maximum energy utilization of the network. This is mainly because of the fact that the forwarding load of nodes near the center increases drastically as the transmission range decreases too much. Another point to mention is that although the node density seems to have no effect on the selection of the optimal T, but it implicitly influences the solution through altering the value of W and $\bar{\theta}$.

Through analyzing the interference function in (7), we can derive that, as much as the transmission range increases, more paths are likely to intersect with transmission disks of nodes and thus the amount of virtual interference increases too. Also, just like $L_f(d)$, $VI(d)$ rises as d tends to zero. In fact, the virtual interference calculated in case (i) (explained in Section 4.2) reaches its summit at the center, and in case (ii), it remains equal for all points of the circle. This can reduce the actual lifetime of the network even more, since as a result of a high interference at the center, more packet loss and hence more packet retransmissions is likely to be triggered, which further depletes the power of hot spots. It is worthy to mention that the emergence of such high load and interference at the centric part of the network mainly roots in the pure usage of shortest paths between nodes, because most of these paths should pass over this small area to reach their destinations. As an example, our analysis shows that about 2/3 of all shortest paths intersect with transmission disk of the center. Therefore, by selecting a better routing, the network lifetime will be improved undoubtedly.

The average forwarding load and virtual interference acquired in the optimal simple strategy (with $T = 1.2$) are plotted in Fig. 7. With a brief look at this figure, we can observe that both the load and the interference become severely high at the center. The results indicate that even using the optimal transmission range cannot yield a good load distribution over the network and still creates a hot spot region with a high interference potential at the center. In Section 6, we also provide simulation results for these two cases which corroborate our analysis.

5. The combined strategy

In the previous section, we argued briefly that the routing is a promising tactic to improve network lifetime. In this section, we try to find a better solution to the SEC problem, through devising a more efficient routing method. A traditional way of solving this problem is linear programming, in which the constraints are topology and routing constraints which are actually flow conservation. However, this approach is applicable only in small networks, because the size of the problem space increases dramatically as the number of nodes grows. Therefore, we rely on heuristics to achieve a better solution.

5.1. Combined shortest path routing and circular routing

Through investigating the distribution of forwarding load in the former strategy, we found out that the peripheral nodes of the network always take a much lighter load than nodes near the center. As a first conclusion, a better strategy should exploit the energy capacity of these nodes to compensate the energy consumption of hot spots.

Our new strategy is schematically depicted in Fig. 8. As the figure shows, the field is divided into two segments: a segment with a concentric circle of radius R_i ($R_i < R$) which we refer to as the *inner circle* (or C_{OR_i}) and an annulus segment between the inner circle and periphery of the network, illustrated by the grayed annulus in Fig. 8. The routing method of the new strategy is devised as follows:
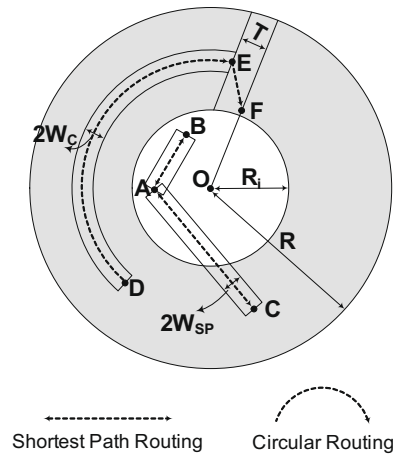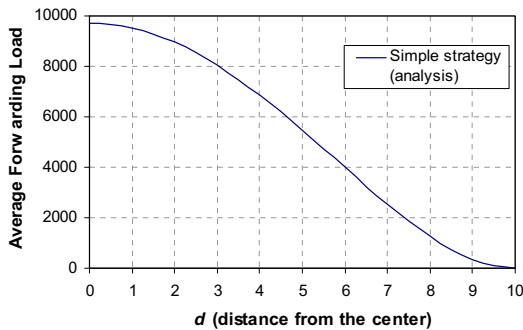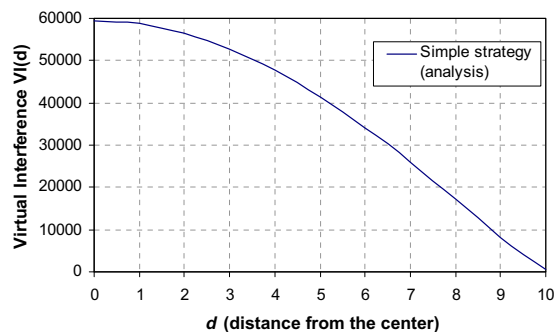

Fig. 8. Combined shortest path routing and circular routing.

(a) Average forwarding load vs. distance from center

(b) Virtual Interference vs. distance from center

Fig. 7. Forwarding load and virtual interference distribution in the simple strategy. We assume $R = 10$, $W = 1$, $\lambda = 1$, $\delta = 2$, and $T = 1.2$.

1. Nodes within C_{OR_i} still take the shortest paths when transmitting data towards other nodes of C_{OR_i}, e.g., the path between A and B in Fig. 8.
2. Also, nodes within C_{OR_i} use the shortest paths for transmitting data towards nodes of the annulus segment, and vice versa, e.g., the path between A and C in Fig. 8.
3. Nodes in the annulus perform a two-step routing to transmit data to other nodes of the annulus. Suppose node D in Fig. 8 wants to communicate with node F. The path from D to F first circles around the center until reaches a node, e.g., node E, whose distance to line OF is less than the transmission range T. We call this step *circular routing* and also node E as *turning node* along the path from D to F. Then, it follows the shortest path from the turning node to the destination (we call this path as *turning path*). The direction of the circular routing depends on the location of source with respect to the destination node: clockwise if node D is laid on one side of line OF and counterclockwise on the other side.

Overall, the rationale behind this combined strategy is that it tries to reduce the number of paths that go over the network's hot spot by confining the network section that applies the SP routing. Based on the rectangle model introduced in Section 4.1, we assume that the shortest paths between nodes (constructed in case 1 and 2 of the above routing) lie inside a rectangle with width of $2W_{SP}$. Also, the circular path used in case 3 can be imagined to be positioned within an annulus with width of $2W_C$ formed around an arc which connects two nodes together (Fig. 8). Just like W_{SP}, the average value of W_C is governed by the node density δ and network radius R and is supposed to be independent of T. We use an approach similar to the one introduced in Section 4.1 to approximate W_C for a given value of δ and R (e.g., we get $W_C = 1.2$, when $\delta = 2$ and $R = 10$). Like the simple strategy, the transmission range of all nodes (whether they are in the inner circle or in the annulus segment) is configured to the same value T in the new strategy too.

It can be inferred from above that the main challenge of the combined strategy is choosing R_i and T deliberately to optimize the maximum energy utilization among nodes. However, to obtain the optimal values of R_i and T, we should develop analytical models to describe properties of nodes in the new strategy too.

An analysis, similar to the one brought up in Section 4.1, can be applied to compute $L_f(d)$ for nodes located within the inner circle (i.e., when $d \leqslant R_i$). Since the radius of this part has reduced from R to R_i, it is easy to show that the maximum load of this part, which occurs at the center, is $(R_i/R)^2$ fraction of the maximum load obtained by the simple strategy; namely:

$$L_f(0) = \left(\frac{R_i}{R}\right)^2 \cdot \frac{R^4}{T^2} \bar{\theta}_i \delta \lambda = \left(\frac{R_i R}{T}\right)^2 \bar{\theta}_i \delta \lambda, \quad (11)$$

where $\bar{\theta}_i$ is the value of $\bar{\theta}$ calculated for the inner circle. Similar to the case of forwarding load, the virtual interference inside C_{OR_i} will be reduced, because all circular paths bypass the central part to reach their destinations. In order to compute $VI(d)$ for these nodes, we can use the same ap-

proach presented in Section 4.2. Following the relation in (7), we have

$$VI(d) = \int \int_{\forall P \in \{C_{OR} - C_{AT}\}} \delta \cdot S_{T,R_i}(A, P) \delta \, dx \, dy + \delta \pi R^2 \times \delta \pi T^2. \quad (12)$$

However, for nodes outside C_{OR_i}, a different analysis should be made, because the rectangle model can not be applied there. If we could characterize the load distribution for this part of the network, we could choose the best value of R_i and T in order to disperse the traffic load efficiently between two segments.

Consider a node A which is at distance d from the center where $d > R_i$. Based on the above combined routing, the forwarding load taken by this node is composed of three major parts: (i) $L_1(d)$, the load of forwarding traffic along the circular paths constructed in case 3 of the combined strategy, (ii) $L_2(d)$, the load of forwarding traffic along the turning paths constructed in case 3, and (iii) $L_3(d)$, the load of forwarding traffic along the shortest paths constructed in case 2. In Appendix II, we present a complete set of relations to compute $L_i(d)$, for $i = 1, 2, 3$.

Just like the forwarding load, the virtual interference of node A is composed of three parts: (i) $VI_1(d)$, the number of circular paths that intersect with C_{AT} (i.e., the transmission disk of A), (ii) $VI_2(d)$, the number of turning paths intersecting with C_{AT}, and eventually (iii) $VI_3(d)$, the number of all shortest paths that intersect with C_{AT}. In Appendix III, we give a detailed explanation about how this model is built.

5.2. How to choose R_i and T?

As described earlier, the choice of R_i and T can significantly influence the performance of the proposed combined strategy. In this section, we present an analytical way to find the best value of R_i and T and then analyze the strategy with respect to the forwarding load and interference parameters.

Since all nodes have the same range, we can simply conclude that the energy consumption rate inside C_{OR_i} gets maximum at the center. Using (8) and (11), this maximum energy can be calculated by

$$E(0) \approx \lambda \left(\left(\frac{R_i R}{T}\right)^2 \bar{\theta}_i \delta + \pi R^2 \delta \right) \cdot (\gamma + \alpha T^n)$$

$$= \delta \lambda R^2 \left(\frac{R_i^2}{T^2} \bar{\theta}_i + \pi \right) \cdot (\gamma + \alpha T^n). \quad (13)$$

Having fixed the value of R_i, we can find the optimal T for minimizing $E(0)$ through taking derivative from (13), similar to the approach we used in Section 4.3. Finally, we get the following equation where the root determines the best value of T:

$$n \pi \alpha T^{n+2} + (n-2) R_i^2 \bar{\theta}_i \alpha T^n - 2R^2 \bar{\theta}_i \gamma = 0. \quad (14)$$

Unfortunately, as Appendix II shows, the forwarding load distribution in the annulus segment has such a complex form that obtaining a simple expression for the optimal R_i and T is hardly possible. However, since our strategy

tries to disperse the forwarding load of hot spot evenly over two segments, we can intuitively argue that the optimal R_i yields the same maximum energy utilization for both segments. Hence, given a certain R_i ($0 \leqslant R_i \leqslant R$), we first find the best value of T that optimizes $E(0)$ by solving (14). Then, we compute the maximum energy consumption in two segments under the chosen T, using the analytical modeling of forwarding load distribution presented in AppendixII. By varying the value of R_i, we can get the optimal values of R_i and T for a given network setting (i.e., for a specific node density and network radius). Although the load and the energy functions have not a closed form, but they are solely functions of δ and R and can be easily evaluated by mathematical tools or simple numerical methods, such as the Monte Carlo method. Here, we emphasize that the computation phase of our strategies is done only once (e.g., at start-up) for each network setting. So, when T and R_i are determined, wireless nodes don't need to compute anything.

Fig. 9 demonstrates the analytical results of the maximum energy consumption with respect to different values of R_i in a network with $R = 10$, $W_{SP} = 1$, $W_C = 1.2$, $\alpha = 1$, $\gamma = 1$, $\lambda = 1$, $\delta = 2$ and $n = 3$. The maximum energy is optimized at $R_i \approx 6$. This selection of R_i leads to $T = 1$ as the best value for T that minimizes $E(0)$. If we had shown the result of selecting different transmission ranges, again it could be observed that the maximum rate of energy utilization does not necessarily reduce as the transmission range decreases.

Through investigating the virtual interference distribution, we can deduce that as T decreases, the virtual interference inside both segments decreases too. In fact, $VI(d)$ for nodes inside C_{OR_i} complies the function in (12) which is reduced when T decreases. Similarly, for nodes outside the circle, decreasing T will reduce all three parts of the virtual interference function. More importantly, due to the usage of circular paths, the combined strategy is expected to notably improve $VI(d)$ at the centric part of the network.

The analytical results of the combined strategy are plotted in Fig. 10. These two diagrams evidently confirm that both load and interference are spread much better over the network, comparing with the results of the simple strategy shown in Fig. 7. Note that characterizing the distribution of forwarding load and virtual interference in the annulus $[R_i - T, R_i + T]$ is very hard, because there is no clear demarcation between two segments that apply different routings. Instead, we solely rely on simulations to find the characteristics of nodes in this area.

5.3. Strategy implementation

Now, we provide a brief discussion on implementation issues of the combined strategy. First, we should mention that the idea of circular routing is not new and has been introduced previously in [34] as a useful way to balance the load of traffic in wireless sensor networks. But, our adoption of circular routing (in the combined strategy) is novel in ad hoc networks. In order to implement this routing, several mechanisms can be used. One way is to use the trajectory based forwarding, proposed in [35,36], which provides a way to shape a routing path into a predefined curve. In our case, the curve is simply an arc parameterized by a radius and center coordinates. Another simple approach to realize this routing could be as follows. Each packet header contains two fields which are filled by the original source: the distance of the source from the center (denoted by d_{src}) and the direction of the circular path between the source and the destination, i.e., clockwise or counterclockwise (denoted by dir). Once a packet arrives at an intermediate node, it forwards the packet on direction dir towards a neighbor whose distance from the center is closest to d_{src} among all its neighbors. In both approaches, the location-awareness is necessary for nodes that apply such a routing, which certainly results in extra overhead. However, in the latter one, only the turning node needs to know the exact location of the destination. The source and also the intermediate nodes along a circular path only have to estimate two kinds of information: (1) whether the destination is inside the inner circle or the annulus segment, and (2) whether direction of the circular path towards destination is clockwise or counterclockwise. This brings some type of localization by which only a small portion of nodes, which are fortunately very close to the destination, need accurate information about the position
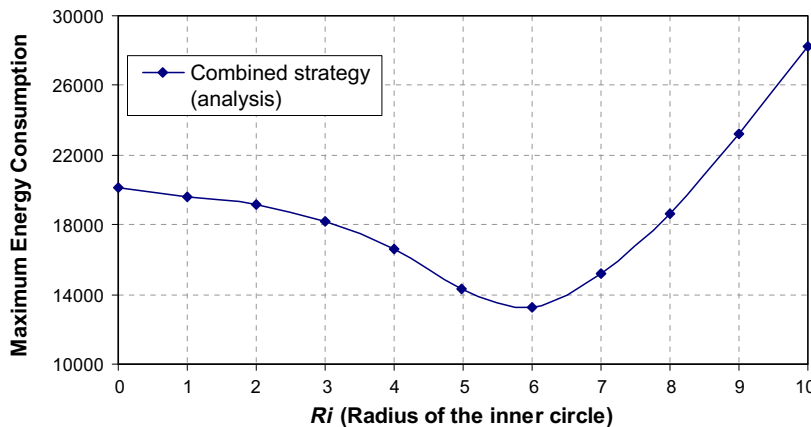

Fig. 9. Maximum energy obtained in combined strategy under different values of R_i.

(a) Average forwarding load vs. distance from center   (b) Virtual Interference vs. distance from center
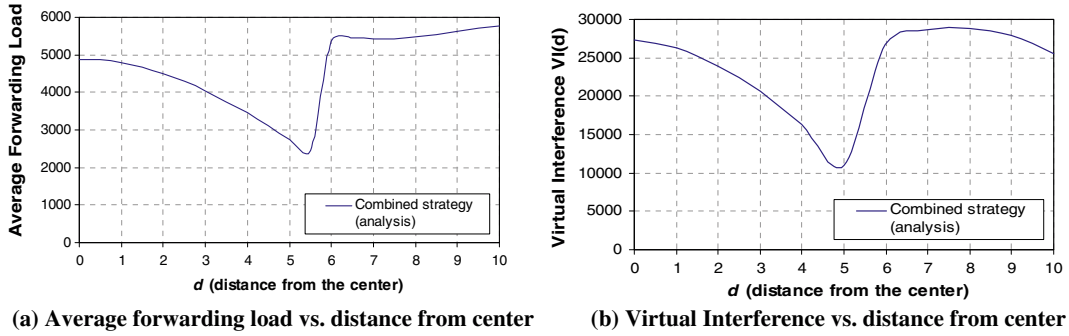
Fig. 10. Forwarding load and virtual interference distribution in the combined strategy. We assume $R = 10$, $\lambda = 1$, $\delta = 2$, $R_i = 6$, and $T = 1$.

of the destination, while other nodes only require to know a restricted positional information which is much more stable.

Although the circular field is the most widely used shape for modeling the network region (and also a good one to estimate other shapes), but this question may arise that "what if the network field is not circular?". The combination of the SP routing and trajectory based routing (shaped based on the periphery of the field) can be speculated as a near optimum solution, as it disperses the traffic flows well over the network. However, calculating the optimal T and R_i depends highly on the shape of the network field, but the idea of exploiting the redundant capacity of peripheral nodes always applies. The final point to mention is that although the value of transmission range in both strategies are determined by solving (10) and (14), but they can't give any guarantee on the connectivity of nodes in the resulted topology. However, there are several analytical methods that approximate the critical transmission range as a function of the network field, node distribution, and density (e.g. [15–17]). Also, some graph based methods have been proposed that determine the exact critical range in a fast and efficient manner for a given placement of nodes (for example, [18]). Since the energy utilization function is known in both strategies, we are able to find the best transmission range that preserves connectivity too.

6. Performance evaluation

In this section, we present the results of simulations we have conducted to evaluate the performance of our strategies. We also compare them with the results of the traditional approach which uses the popular shortest path routing and assigns the critical transmission range to all network nodes.

6.1. Simulation environment

Our experiments were carried out using a customized high level simulator implemented in C++. The simulation setups are as follows: The radius of the network field is set to $R = 10$ while nodes are uniformly distributed inside the circle with density $\delta = 2$. In each experiment, after generating a placement of nodes, we first construct the net-

work topology in both strategies and then run the appropriate routing method (i.e., the shortest path routing or the combined one) on the resulted network consisting of those nodes. For each strategy, we measure the forwarding load, the interference and the energy consumption of nodes according to their distance from the center. We assume that the rate of energy consumption in each node is computed according to (5) with $\alpha = 1$, $\gamma = 1$, and $n = 3$. Also, we fix the average traffic rate λ to 1. Note that, although our strategies have been designed to run in a distributed manner, our simulations assume a static discipline. That is, given a random placement of nodes, we run each of strategies statically on the network to find routing paths between nodes. For each strategy, we perform 10 simulations with different node placement.

6.2. The simple strategy

First, we present the results of the experiments we have done for the simple and traditional strategies. Fig. 11 shows the results of the maximum energy consumption obtained under different values of T in the simple strategy. One can easily see the similarity between this plot and that of Fig. 6. The difference between these two diagrams is mainly due to the fact that the computation of forwarding load in Fig. 6 is based on approximation which assumes a perfect load balanced routing. Despite this error, the overall tendency is valid. For example, the maximum energy consumption is optimized at $T \approx 1.4$ which is near to the one achieved through analysis (i.e., $T \approx 1.2$).

Fig. 12 compares the results of the simple strategy with those of the traditional one. The figure represents the average forwarding load and interference of nodes versus their distance from the center. The analytical results are simply a re-plot of the curves in Fig. 7. As we can see there, simulation results of the simple strategy match analytical ones very well in terms of the average forwarding load. Note that when d goes beyond 5, the difference between two results becomes slightly larger; the reason is that we have applied the $\bar{\theta}$ estimation of the center for every other node. In the case of virtual interference, analytical results appear to be rather pessimistic (about 10% higher, on average). This is because we have considered the virtual interference in our analysis while simulations take the actual interference into account. Recall that the virtual interference of a
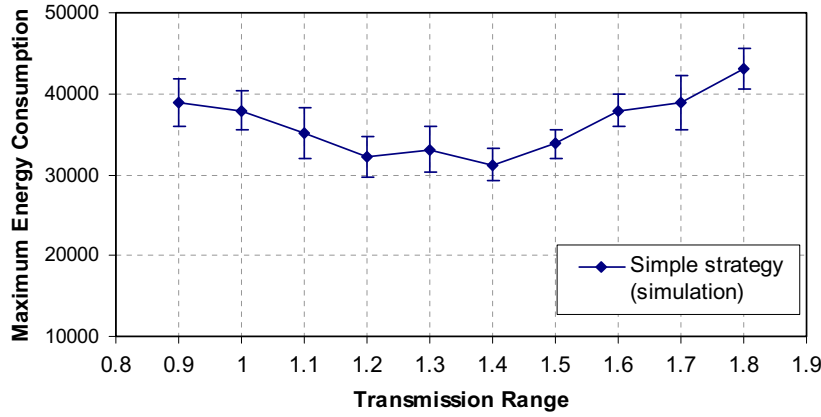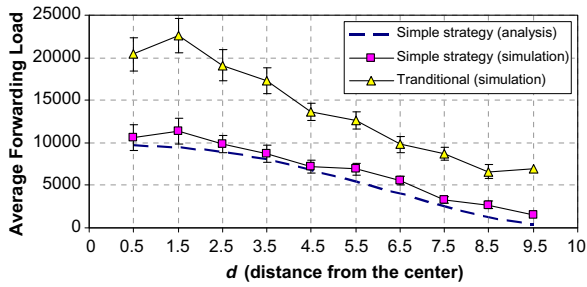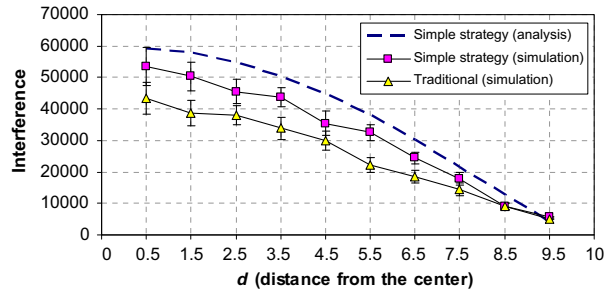
Fig. 11. Maximum energy obtained in the simple strategy under different values of the transmission range *T*.

(a) Average forwarding load vs. distance from center

(b) Interference vs. distance from center

Fig. 12. Forwarding load and interference distribution in the simple strategy. We set *T* = 1.2 and *T* = 0.8 for simple and traditional strategies, respectively.

node is computed based on the number of paths that only <u>intersect</u> with the transmission disk of the node. So, it is reasonably higher than the actual interference which is calculated based on the number of paths that pass over the <u>coverage set</u>. Nonetheless, the analytical results can properly show the relative interference of the network nodes.

A simple comparison between the experimental results of two strategies in Fig. 12 reveals that the simple strategy yields a much lower forwarding load (50%, on average) than the traditional one. The reason is that when the transmission range gets smaller, the routing paths should pass over more hops to get to their destinations, and this evidently increases the load on intermediate nodes. On the other hand, as a result of selecting a lower range, the traditional strategy brings a better result with respect to the interference (around 15%, on average). Bear in mind that based on (7), interference has a reverse relation with transmission range which is confirmed by the above results, as well.

6.3. The combined strategy

Now, we provide simulation results for the proposed combined strategy. Fig. 13 displays the results of the maximum energy consumption obtained by this strategy when R_i varies from 0 to 10. The value of *T* is selected analytically
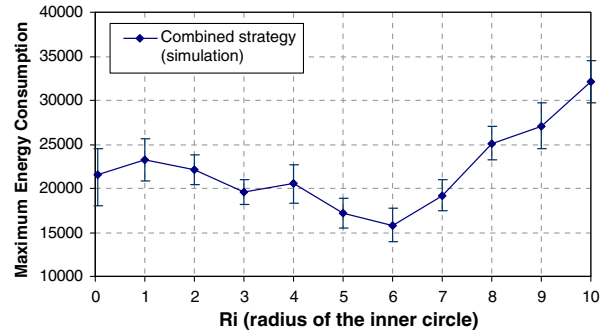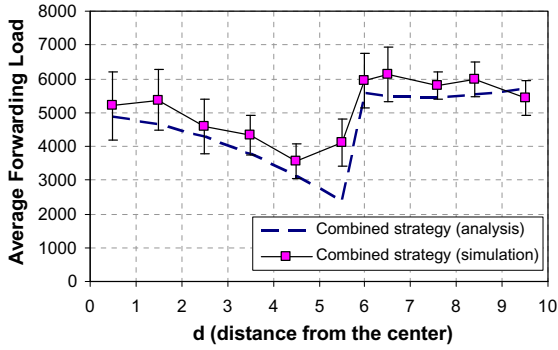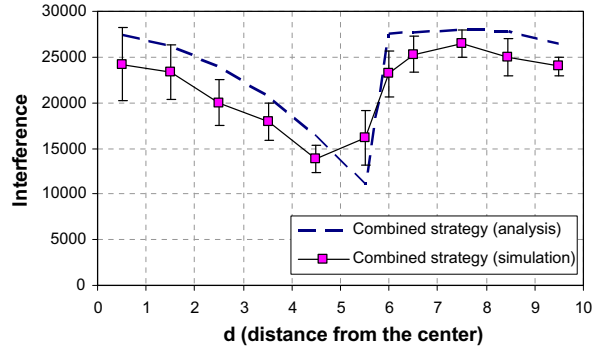

Fig. 13. Maximum energy obtained in the combined strategy under different values of R_i.

in a way that the maximum energy consumption in both segments $[0, R_i]$ and $[R_i, R]$ is minimized. As the figure shows, the lowest value of maximum energy is obtained at $R_i = 6$, which gives us the best choice of the strategy. This value is the same as the one obtained through analysis and hence, it confirms the validity of our model. Also, a simple comparison between Figs. 11 and 13 shows that the combined strategy has succeeded to reduce the maximum consumed energy by about 50%, in comparison with the simple strategy.

(a) Average forwarding load vs. distance from center

(b) Interference vs. distance from center

Fig. 14. Forwarding load and interference distribution in the combined strategy. We assume $R_i = 6$, and $T = 1$.

At last, Fig. 14 compares the simulation results of combined strategy with the analytical ones for the case that we have chosen $R_i = 6$ and $T = 1$, which are the optimal values according to our analysis. The figure represents the average forwarding load and interference of nodes versus their distance from the center. The analytical results are borrowed from the curves in Fig. 10. As it can be seen there, the results of forwarding load obtained through simulation match the analytical ones well. However, as we expected beforehand, the difference between two results gets large when $R_i - T \leqslant d \leqslant R_i + T$, (i.e., inside the annulus $[R_i - T, R_i + T]$). However, the actual interference of nodes obtained by simulation is on average 10% smaller than their corresponding virtual interference (Fig. 14b).

By evaluating the results of both strategies, shown in Figs. 12 and 14, we observe that the combined strategy has significantly reduced the forwarding load and interference of the central region by about 50%, in comparison with the simple counterpart. Indeed, it improves both parameters in the inner circle, at the cost of an increased load and interference in the annulus segment. As the first consequence, the network lifetime in the combined strategy is expected to be at least twice as long as the one obtained in the simple strategy. The maximum load and interference of two segments become roughly equal when $R_i = 6$, and this again confirms our selection of $R_i = 6$ as the best choice of the strategy.

7. Conclusion

In this paper, we considered a novel energy conservation problem in wireless ad hoc networks that takes both transmission range and traffic load of nodes into account to elongate network lifetime. We first introduced our simple strategy in which one single transmission range is assigned to all nodes of the network so that the maximum rate of energy utilization becomes optimum under the assumption of using the shortest path routing. The results of this strategy showed that nodes located close to the center suffer from premature battery depletion, leading to an early network failure. These results suggested that routing is indeed a promising tactic that deserves to be considered when maximizing the network lifetime. In particular, we

proposed using circular paths along with shortest paths to better exploit the energy capacity of nodes at the periphery of the network and reduce the load of hot spots. This combined strategy achieves a nearly 50% improvement in terms of traffic load, interference and energy consumption in hot spots, compared with the simple strategy. For all these scenarios, we developed analytical models, corroborated by a set of simulations.

Appendix I. Estimation of forwarding load in simple strategy

Here, we present an analytical way for calculating the average forwarding load of the nodes in the simple strategy. Consider Fig. 15. Based on the approach introduced in Section 4.1, we are going to find a sector $\bar{S}_3$ with angle $\bar{\theta}$ that is equivalent to S_2 on average and is decoupled from d_{AP}. Since $|S_3|$ is mostly dependent on its height, i.e., d_{AD}, rather than θ (since $| S_3 | \approx d_{AD}^2 \theta / 2$), we compute $\bar{\theta}$ when A is placed at the center and then apply this value as an estimation for every node A. Let $S_2(d)$ be the sum of the values of $|S_2|$ for all points $P \in C_{OR}$ and a point A which is at distance d from O. Also, assume that $S_3(d)$ is the sum over all values of $|S_3|$. We want $S_2(d) = S_3(d)$ for $d = 0$. When A is placed at the center, we can calculate $S_3(0)$ simply by:
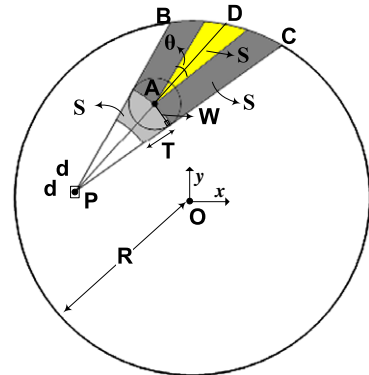

Fig. 15. Approximating the area S_2 by the area S_3.

$$S_3(0) = \int_{\alpha=0}^{2\pi} \int_{r=0}^{R} |S_3| \cdot r \cdot dr \cdot d\alpha$$
$$= \int_{\alpha=0}^{2\pi} \int_{r=0}^{R} \frac{1}{2} R^2 \bar{\theta} \cdot r \cdot dr \cdot d\alpha = \frac{1}{2} \pi R^4 \bar{\theta}. \qquad (15)$$

Also, we can use the following relation to compute $S_2(0)$:

$$S_2(0) = \int_{\alpha=0}^{2\pi} \int_{r=0}^{R} |S_2| \cdot r \cdot dr \cdot d\alpha$$
$$= \int\int_{\forall B \in C_{OR} - C_{OW}} \left(S_{W,R}(O,B) + \frac{1}{2}\pi W^2 \right) \cdot r \cdot dr \cdot d\alpha$$
$$+ \int\int_{\forall B \in C_{OW}} \frac{1}{2}\pi R^2 \cdot r \cdot dr \cdot d\alpha, \qquad (16)$$

where the first and the second term in the above sum formulize $|S_2|$ for the cases in which $d_{AP} > W$ and $d_{AP} \leqslant W$, respectively. Let $S_2(0) = S_3(0)$, and assume that $R = 10$, $W = 1$, and $\delta = 2$; thus, we have $\bar{\theta} = 0.7$. The value of W has been approximated through experiment by averaging among all paths in a graph formed by $T_{min} \approx 0.8$. The average W remains rather the same for other values of T.

On the other hand, $|S_1|$ can be estimated by $\pi T^2/2$. Considering the above simplified model, the amount of load on A for forwarding traffic flows towards P, denoted by $L_f(A,P)$, will be

$$L_f(A,P) = \frac{|S_2|}{|S_1|}\delta\lambda \approx \frac{|S_3|}{|S_1|}\delta\lambda \approx \frac{\bar{\theta} \cdot d_{AD}^2}{\pi T^2}\delta\lambda, \qquad (17)$$

where D is the intersection point of line AP and circle C_{OR} within the sector S_3.

Let us now compute the total forwarding load of node A. As shown in Fig. 16, consider that node A is charged with the forwarding of all traffic flows from S_3 toward nodes inside a very small sector S_4; the areas S_3 and S_4 are centered around line AP with an angle of $\bar{\theta}$ and $d\alpha$, respectively, and D and E are two intersection points of line AP with C_{OR}. As described before, if the value of $\bar{\theta}$ is appropriately chosen, then this model is roughly equivalent with the original one, introduced by Ganjali and Keshavarzian [6], for any position of A. Now, we calculate the total forwarding load of node A by taking a sum over all values of α. For simplification, we assume that $|S_3| \approx \frac{1}{2}d_{AD}^2\bar{\theta}$ and $|S_4| \approx \frac{1}{2}d_{AE}^2 d\alpha$. Considering the fact that $d_{AD} \times d_{AE} = (R^2 - d^2)$, we can
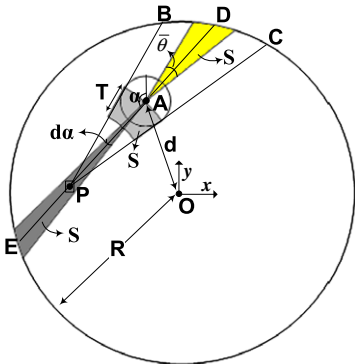

Fig. 16. Estimation of forwarding load $L_f(d)$ in the simple strategy.

derive the following important relation as a closed form expression for $L_f(d)$:

$$L_f(d) \approx \sum_{\alpha=0}^{2\pi} \frac{|S_3|}{|S_3|} |S_4| \delta\lambda \approx \int_0^{2\pi} \frac{\frac{1}{2}d_{AD}^2\bar{\theta}}{\frac{1}{2}\pi T^2} \times \frac{1}{2}d_{AE}^2 d\alpha \cdot \delta\lambda$$
$$= \int_0^{2\pi} \frac{d_{AD}^2 \times d_{AE}^2}{2\pi T^2}\bar{\theta}d\alpha \cdot \delta\lambda$$
$$= \int_0^{2\pi} \frac{(R^2 - d^2)^2}{2\pi T^2}\bar{\theta}d\alpha \cdot \delta\lambda = \frac{(R^2 - d^2)^2}{T^2}\bar{\theta}\delta\lambda. \qquad (18)$$

Recall that based on our simplified model, the value of $\bar{\theta}$ is the same for all nodes of the network and can be approximated by solving the equation $S_2(0) = S_3(0)$.

Appendix II. Computation of forwarding load in combined strategy

In this section, we present a mathematical method for computation of forwarding load in the combined strategy for nodes settled outside C_{OR_i}. Let A be a node at distance d from the center where $d > R_i$. As we explained in Section 5, the forwarding load of node A has three main parts $L_1(d)$, $L_2(d)$, and $L_3(d)$.

$L_1(d)$ is the load of forwarding traffic along the circular paths constructed in the first step of circular routing. Let $x(i)$ be a point on the periphery of the circle C_{OR} such that the angle between line $Ox(i)$ and OA is equal to i. Consider a tiny sector $S_\alpha(d\alpha)$ with a central angle $d\alpha$ around the radius $Ox(\alpha)$, as shown in Fig. 17a. According to the figure, for every destination node P within $S_\alpha(d\alpha)$ that $d_{OP} > d$, the locus of a point B whose circular path towards P goes through A is approximately an annulus formed between the line OA and $Ox(\pi + \alpha)$ with width of $2W_C$, i.e., the area S_2 in Fig. 17a. Similar to the SP routing, we can assume that the load will be shared among nodes in the one-hop area S_1. Hence, the amount of traffic imposed on A by the usage of circular paths towards nodes inside $S_\alpha(d\alpha)$, denoted by $L_1^\alpha(d)$, can be calculated by

$$L_1^\alpha(d) = \frac{S_2\delta \times S_\alpha(d\alpha)\delta}{S_1\delta}\lambda$$
$$= \frac{\frac{(R^2 - R_i^2)d\alpha}{2} \times \frac{((d+W_C)^2 - (d-W_C)^2)(\pi-\alpha)}{2}}{2W_C T}\lambda\delta. \qquad (19)$$

Since the traffic is bi-directional, and is assumed to be the same in both ways (clockwise and counterclockwise), then by taking integration for $d\alpha$ from 0 to π, the total amount of $L_1(d)$ is

$$L_1(d) = 2 \times \int_0^\pi \frac{S_2 \times S_\alpha(d\alpha)}{S_1}$$
$$= 2 \times \int_0^\pi \frac{\frac{((d+W_C)^2 - (d-W_C)^2)(\pi-\alpha)}{2} \times \frac{(R^2 - R_i^2)d\alpha}{2}}{2W_C T}\lambda\delta$$
$$= 2 \times \frac{\frac{1}{8}\pi^2((d+W_C)^2 - (d-W_C)^2)(R^2 - R_i^2)}{2W_C T}\lambda\delta$$
$$= \frac{4\pi^2 W_C d(R^2 - R_i^2)}{8W_C T}\lambda\delta = \frac{d(R^2 - R_i^2)}{2T}\pi^2\lambda\delta. \qquad (20)$$

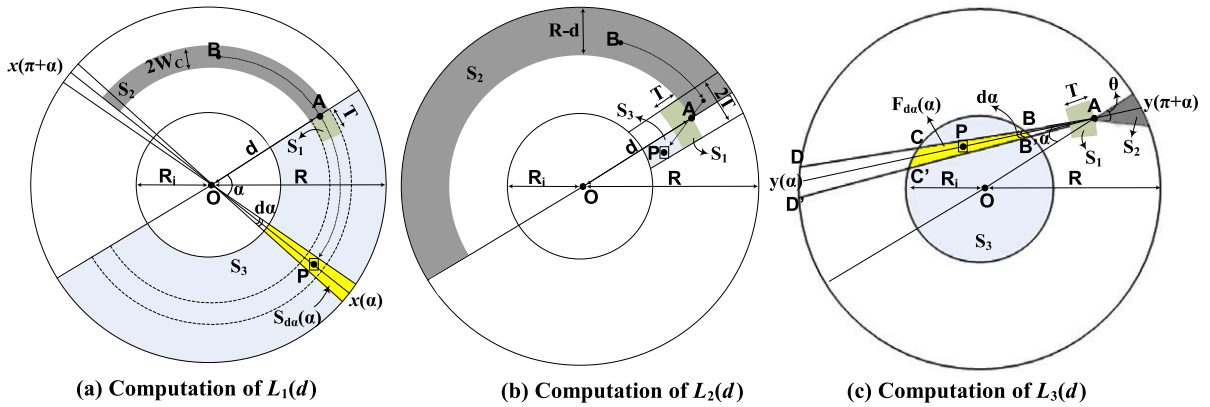**(a) Computation of $L_1(d)$**   **(b) Computation of $L_2(d)$**   **(c) Computation of $L_3(d)$**

Fig. 17. Computation of forwarding load distribution for nodes outside the inner circle in the combined strategy.

On the other hand, $L_2(d)$ is the load due to forwarding traffic along the turning paths constructed in the second step of circular routing. To simplify our analysis, we assume that the turning path is close to the straight line which connects turning node to destination. Consider a source node B and a destination node P. If the turning path from B to P goes through A, then one of the following two cases has happened: (1) the distance between P and line OA is smaller than T, $d_{OB} > d$, and $d_{OP} \leqslant d$, or (2) the distance between P and line OA is smaller than T, $d_{OB} \leqslant d$, and $d_{OP} > d$. These cases are straightforwardly derived from the definition of the combined routing presented in Section 5.1 Notice that we here ignore the impact of W_C on load of nodes, because W_C has roughly a symmetric effect on it. As Fig. 17b illustrates, case 1 leads us to the area S_2 and S_3 as the locus of nodes B and P, respectively. Using a rectangle to approximate $|S_3|$, we have $S_2 = \frac{\pi}{2}(R^2 - d^2)$ and $S_3 = (d - R_i)T$. The locus of node B and P in case 2 can be obtained in a similar manner. Note that the turning paths from S_2 to S_3 will definitely go over the one-hop area S_1 where $S_1 \approx 2T^2$. Since we have assumed that the traffic in both ways is the same, the total amount of $L_2(d)$ is computed by

$$L_2(d) = 2$$
$$\times \frac{\left(\frac{1}{2}\pi(R^2 - d^2)(d - R_i)T^2 + \frac{1}{2}\pi(d^2 - R_i^2)(R - d)T\right)}{2T^2}\delta\lambda$$
$$= \frac{(R^2 - d^2)(d - R_i) + (d^2 - R_i^2)(R - d)}{2T}\pi\delta\lambda$$
$$= \frac{(R - d)(d - R_i)(R + R_i + 2d)}{2T}\pi\delta\lambda.$$
$$(21)$$

Also, $L_3(d)$ is the load of forwarding traffic over the shortest paths constructed between nodes of two segments, namely the inner circle and the annulus segment. In this case, either the source or destination has been placed inside C_{OR_i}, while another one in the annulus. Consider a destination node P inside C_{OR_i}. Let $y(i)$ be a point on the edge of the circle C_{OR} such that the angle between the line $Ay(i)$ and the axis OA is equal to i. Consider $F_\alpha(d\alpha)$ as the portion of the disk formed around $Ay(\alpha)$ inside C_{OR_i} with an aperture of $d\alpha$ (Fig. 17c). Our aim is to determine the amount of traffic destined for nodes inside $F_\alpha(d\alpha)$ which are going through A. For

every destination node P inside $F_\alpha(d\alpha)$, the locus of all points B whose shortest paths towards P go through A is approximately an area centered around $Ay(\pi + \alpha)$ with an aperture of $\bar{\theta}$, i.e., the area S_2 in Fig. 17c. Hence, the amount of traffic load imposed on A by the usage of shortest paths towards nodes inside $F_\alpha(d\alpha)$, denoted by $L_3^\alpha(d)$, is obtained by

$$L_3^\alpha(d) = \frac{S_2 \cdot F_\alpha(d\alpha)}{S_1}\delta\lambda, \tag{22}$$

where $S_1 \approx \frac{\pi}{2}T^2$ and $S_2 \approx \frac{\bar{\theta}}{2} \cdot d_{Ay(\pi+\alpha)}^2$. Let S be the area of the semi-sector DAD' in Fig. 17c which is centered around $Ay(\alpha)$ with an aperture of $d\alpha$. Since $d\alpha$ is very small, we have $S \approx \frac{1}{2} \times d_{Ay(\alpha)}^2 \cdot d\alpha$. On the other hand, we can model the semi-sector DAD' as a right triangle, as depicted in Fig. 18. Through this simplification, it is easy to show that:

$$F_\alpha(d\alpha) = \left(\frac{d_{AC}^2}{d_{AD}^2} - \frac{d_{AB}^2}{d_{AD}^2}\right) \cdot S$$
$$\approx \frac{1}{2} \times \left(\frac{d_{AC}^2}{d_{AD}^2} - \frac{d_{AB}^2}{d_{AD}^2}\right)d_{Ay(\alpha)}^2 \cdot d\alpha, \tag{23}$$

where d_{AD}, d_{AC}, and d_{AB} are obtained from the general relations of crossing a line and a circle, i.e.:

$$d_{AD} = \left|\sqrt{R^2 - d^2\sin^2(\alpha)} + d\cos(\alpha)\right|,$$
$$d_{AC} = \left|\sqrt{R_i^2 - d^2\sin^2(\alpha)} + d\cos(\alpha)\right|, \tag{24}$$
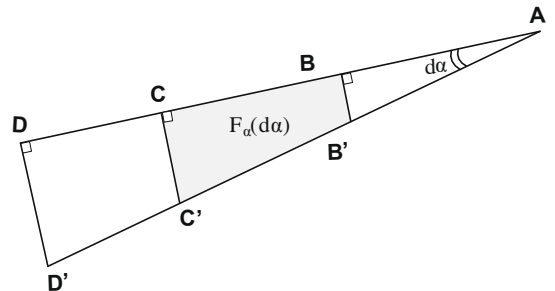$$d_{AB} = \left|\sqrt{R_i^2 - d^2\sin^2(\alpha)} - d\cos(\alpha)\right|.$$

Fig. 18. Calculation of $F_\alpha(d\alpha)$.

Combining (23) and (24), we have

$$L_3^{\alpha}(d) = \frac{1}{4} \times \left(\frac{d_{AC}^2}{d_{AD}^2} - \frac{d_{AB}^2}{d_{AD}^2}\right) \cdot \frac{d_{Ay(\pi+\alpha)}^2 d_{Ay(\alpha)}^2}{0.5\pi T^2} \cdot \bar{\theta}\delta\lambda d\alpha$$

$$= \frac{1}{2} \times \left(\frac{d_{AC}^2}{d_{AD}^2} - \frac{d_{AB}^2}{d_{AD}^2}\right) \cdot \frac{(R^2 - d^2)^2}{\pi T^2} \cdot \bar{\theta}\delta\lambda d\alpha. \quad (25)$$

Again, assuming that the traffic in two ways (i.e., from the inner circle to the annulus and vice versa) is the same, we can compute $L_2(d)$ according to the following relation:

$$L_3(d) = 2 \times \int_{-\sin^{-1}(R_i/d)}^{\sin^{-1}(R_i/d)} L_3^{\alpha}(d) \cdot d\alpha$$

$$= \int_{-\sin^{-1}(R_i/d)}^{\sin^{-1}(R_i/d)} \left(\frac{d_{AC}^2}{d_{AD}^2} - \frac{d_{AB}^2}{d_{AD}^2}\right) \cdot \frac{(R^2 - d^2)^2}{\pi T^2}\bar{\theta}\lambda\delta \cdot d\alpha. \quad (26)$$

Finally, the total forwarding load on node A is achieved by summing $L_1(d)$, $L_2(d)$, and $L_3(d)$ together:

$$L_f(d) = L_1(d) + L_2(d) + L_3(d), \quad d > R_i \quad (27)$$

Appendix III. Computation of virtual interference in combined strategy

This section shows how to compute the virtual interference in the combined strategy for nodes placed outside the inner circle. First, we should mention that like the simple strategy we here ignore the impact of W_{SP} and W_C on the virtual interference of nodes. Let A be a node at distance d from the center where $d > R_i$. Similar to the case of forwarding load, the virtual interference of node A is composed of three major parts $VI_1(d)$, $VI_2(d)$, and $VI_3(d)$.

$VI_1(d)$ is the number of circular paths, constructed in the first step of circular routing, which intersect with C_{AT} (i.e., the transmission disk of A). According to Fig. 19a, for every destination node P inside $S_\alpha(d\alpha)$, the locus of all points B whose circular paths towards P intersect with C_{AT} is approximately an annulus with width of $2T$ between the line OA and $Ox(\pi + \alpha)$, i.e., the area S_1 in Fig. 19a. Following the approach presented in Appendix II, $VI_1(d)$ is computed by

$$VI_1(d) = 2 \times \int_0^{\pi} \frac{((d+T)^2 - (d-T)^2)\delta}{2}$$

$$\times \frac{\delta(R^2 - R_i^2)(\pi - \alpha)d\alpha}{2}$$

$$= \pi^2 dT(R^2 - R_i^2)\delta^2. \quad (28)$$

On the other hand, $VI_2(d)$ is the number of turning paths, constructed in the second step of circular routing, which intersect with C_{AT}. Consider a source node B and a destination node P. If the turning path from B to P intersects the transmission disk of A, then one of the following cases has certainly occurred: (1) the distance between P and the line OA is smaller than T, $d - T < d_{OB} \leqslant R$, and $d_{OP} < d - T$, or (2) the distance between P and the line OA is smaller than T, $R_i < d_{OB} \leqslant d + T$, and $d_{OP} > d + T$. As Fig. 19b shows, case 1 leads to the areas S_1 and S_2 as the locus of node B and P, respectively. The locus of A and P in case 2 can be obtained in a similar manner. For the sake of simplicity, we assume that all paths from nodes inside S_1 to S_2 intersect with the transmission disk of A. This simplification gives us an upper bound on the virtual interference of nodes in the combined strategy. As a result, $VI_2(d)$ can be simply estimated by $S_1 \times (S_2 + \pi T^2)$, where S_2 itself can be approximated using the rectangle model. However, as depicted in Fig. 19, some portion of $VI_2(d)$ calculated in this manner overlaps with $VI_1(d)$. After subtracting this shared area, we have

$$VI_2(d) = \pi(R^2 - (d-T)^2) \cdot (2T \cdot (d-T-R_i))\delta^2$$

$$+ \pi((d+T)^2 - R_i^2) \cdot (2T \cdot (R-d-T))\delta^2$$

$$+ \pi^2 T^2(R^2 - R_i^2)\delta^2 - 4\pi T^2 d(R - R_i)\delta^2 \quad (29)$$

Finally, $VI_3(d)$ is the number of shortest paths, constructed between nodes of two segments, which intersect with C_{AT}. In this case, one of the source and destination nodes has been placed inside C_{OR_i} while another one in the annulus segment. Consider a destination node P inside C_{OR_i}. From Fig. 19c, it is apparent that the locus of all points B whose shortest paths towards P intersect with the transmission disk of A is the combination of $S_{T,R}(A,P)$ and C_{AT}.

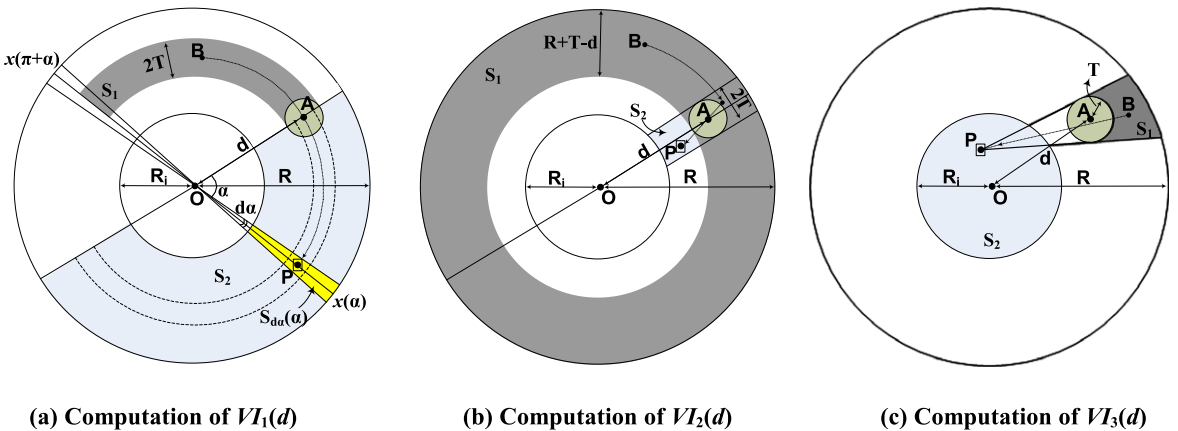(a) Computation of $VI_1(d)$ (b) Computation of $VI_2(d)$ (c) Computation of $VI_3(d)$

Fig. 19. Virtual interference distribution for nodes outside the inner circle in the combined strategy.

Considering all points P inside C_{OR_i} and assuming that the shortest paths in two ways (i.e., from the inner circle to the annulus and vice versa) are the same, we will have

$$VI_3(d) = 2 \times \int \int_{\forall P \in C_{OR_i}} \delta \cdot S_{T,R_i}(A,P) \delta\, dx\, dy + \delta \pi R_i^2 \times \delta \pi T^2 \tag{30}$$

and we conclude.

References

[1] C.E. Jones, K.M. Sivalingam, P. Agrawal, J.C. Chen, A survey of energy efficient network protocols for wireless networks, Wireless Networks 7 (4) (2001) 343–358.

[2] M. Hempstead, N. Tripathi, P. Mauro, G.Y. Wei, D. Brooks, An ultra low power system architecture for sensor network applications, in: Proc of. ISCA, 2005.

[3] H. Liu, T. Roeder, K. Walsh, R. Barr, E.G. Sirer, Design and implementation of a single system image operating system for ad hoc networks, in: Proc. of Mobisys, 2005.

[4] E.L. Lloyd, R. Liu, M.V. Marathe, R. Ramanathan, S.S. Ravi. Algorithmic aspects of topology control problems for ad hoc networks, in: Proc. of ACM MobiHoc, 2002.

[5] P. Santi, D.M. Blough, F. Vainstein, A probabilistic analysis for the range assignment problem in ad hoc networks, in: Proc. of ACM MobiHoc, 2001.

[6] Y. Ganjali, A. Keshavarzian, Load balancing in ad hoc networks: single-path routing vs. multi-path routing, in: Proc. of IEEE INFOCOM, 2004.

[7] R. Ramanathan, R. Rosales-Hain, Topology control of multihop wireless networks using transmit power adjustment, in: Proc. of IEEE INFOCOM, 2000.

[8] R. Wattenhofer, L. Li, P. Bahl, Y. Wang, Distributed topology control for power efficient operation in multihop wireless ad hoc networks, in: Proc. of IEEE INFOCOM, Alaska, 2001.

[9] S. Narayanaswamy, V. Kawadia, R.S. Sreenivas, P.R. Kumar, Power control in ad-hoc networks: theory, architecture, algorithm and implementation of the COMPOW protocol, in: Proc. of European Wireless 2002, Next Generation Wireless Networks: Technologies, Protocols, Services and Applications, Florence, Italy, February 2002.

[10] V. Kawadia, P.R. Kumar, Power control and clustering in ad hoc networks, in: Proc. of IEEE INFOCOM, 2003.

[11] X. Li, W. Song, W. Wang, A unified energy-efficient topology for unicast and broadcast, in: Proc. of ACM Mobicom, 2005.

[12] N. Li, J.C. Hou, Localized topology control algorithms for heterogeneous wireless networks, IEEE/ACM Transactions on Networking 13 (6) (2005) 1313–1324.

[13] N. Li, J.C. Hou, Localized fault-tolerant topology control in wireless ad hoc networks, IEEE/ACM Transactions on Parallel and Distributed Systems 17 (4) (2006) 307–320.

[14] W. Song, X. Li, O. Frieder, W. Wang, Localized topology control for unicast and broadcast in wireless ad hoc networks, IEEE/ACM Transactions on Parallel and Distributed Systems 17 (4) (2006) 321–334.

[15] P. Santi, D. Blough, The critical transmitting range for connectivity in sparse wireless ad hoc networks, IEEE Transactions on Mobile Computing 2 (1) (2003).

[16] P. Wan, C. Yi, Asymptotic critical transmission radius and critical neighbor number for k-connectivity in wireless ad hoc networks, in: Proc. of ACM MobiHoc, 2004.

[17] J. Deng, Y. Han, P. Chen, P. Varshney, Optimum transmission range for wireless ad hoc networks, in: Proc. of IEEE WCNC, 2004.

[18] Q. Dai, J. Wu, Computation of minimal uniform transmission range in ad hoc wireless networks, Springer Cluster Computing Journal 8 (2005).

[19] Vincent D. Park, M. Scott Corson, A highly adaptive distributed routing algorithm for mobile wireless networks, in: Proc. of IEEE INFOCOM, Japan, 1997.

[20] David B. Johnson, David A. Maltz, Yih-Chun Hu, The dynamic source routing protocol for mobile ad hoc networks (DSR), Internet Draft, IETF Mobile Ad hoc Networks (MANET) Working Group.

[21] Charles E. Perkins, Elizabeth M. Belding-Royer, Samir R. Das, Ad hoc on-demand distance vector (AODV) routing, Internet Draft, IETF Mobile Ad hoc Networks (MANET) Working Group.

[22] C. Perkins, P. Bhagwat, Highly dynamic destination-sequenced distance-vector Routing (DSDV) for mobile computers, in: Proc. of ACM SIGCOMM, UK, 1994.

[23] S.R. Das, C.E. Perkins, E.M. Royer, Performance comparison of two on-demand routing protocols for ad hoc networks, in: Proc. of IEEE INFOCOM, Israel, 2000.

[24] P. Johansson, T. Larsson, N. Hedman, B. Mielczarek, M. Degermark, Scenario-based performance analysis of routing protocols for mobile ad hoc networks, in: Proc. of ACM Mobicom, 1999.

[25] V. Rodoplu, T.H. Meng, Minimum energy mobile wireless networks", IEEE Journal of Selected Areas in Communications 17 (8) (1999) 333–1344.

[26] S. Singh, M. Woo, C.S. Raghavendra, Power-aware routing in mobile ad hoc networks, in: Proc. of ACM Mobicom, 1998.

[27] O. Savas, M. Alanyali, B. Yener, Joint route and power assignment in asynchronous multi-hop wireless networks, in: Proc. of MedHocNet, June 2004.

[28] Y. Li, A. Ephremides, A joint scheduling, power control and routing algorithm for ad hoc wireless networks, Elsevier Ad Hoc Networks 5 (7) (2007) 959–973.

[29] J. Pan, Y.T. Hou, L. Cai, Y. Shi, S.X. Shen, Topology control for wireless sensor networks, in: Proc. of ACM Mobicom, 2003.

[30] P.P. Pham, Sylvie Perreau, Performance analysis of reactive shortest path and multi-path routing mechanism with load balance, in: Proc. of IEEE INFOCOM, 2003.

[31] J.H. Chang, L. Tassiulas, Energy conserving routing in wireless ad-hoc networks, in: Proc. of IEEE INFOCOM, 2000.

[32] E.J. Duarte-Melo, M. Liu, A. Misra, A modeling framework for computing lifetime and information capacity in wireless sensor networks, in: Proc. of WiOpt, 2004.

[33] J. Gao, L. Zhang, Load balanced short path routing in wireless networks, in: Proc. of IEEE INFOCOM, 2004.

[34] J. Luo, J.P. Hubaux, Joint mobility and routing for lifetime elongation in wireless sensor networks, in: Proc. of IEEE INFOCOM, 2005.

[35] D. Niculescu, B. Nath, Trajectory based forwarding and its applications, in: Proc. of ACM Mobicom, 2003.

[36] M. Yuksel, R. Pradhan, S. Kalyanaraman, An implementation framework for trajectory-based forwarding in ad-hoc networks, in: Proc. of IEEE ICC, 2004.

Sajjad Zarifzadeh received the B.S. and M.S. degrees in Computer Science and Engineering from University of Tehran, Tehran, Iran, in 2002 and 2005, respectively. He is currently working as a research assistant in the Router Laboratory, University of Tehran. His main research interests include network algorithms, specially routing and topology management.

Amir Nayyeri received the B.S. and M.S. degrees in Computer Science and Engineering from University of Tehran, Tehran, Iran, in 2004 and 2007, respectively. He is currently pursuing his PhD in Computer Science in University of Illinois at Urbana Champaign, USA. His main research interests include theoretical computer science.
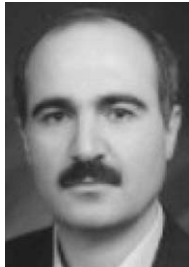
Nasser Yazdani got his B.S. degree in Computer Engineering from Sharif University of Technology, Tehran, Iran. He worked in Iran Telecommunication Research Center (ITRC) as a researcher and developer for few years. To pursue his education, he entered to Case Western Reserve Univ., Cleveland, Ohio, USA, later and graduated as a Ph.D. in Computer Science and Engineering. Then, he worked in different companies and research institutes in USA. He joined the ECE Dept. of Univ. of Tehran, Tehran, Iran, as an Assistant Professor in September 2000. His research interest includes networking, packet switching, access methods, operating systems and database systems.

Hamid Hajabdolali Bazzaz obtained his B.S. in Computer Science and Engineering from University of Tehran, Tehran, Iran in September 2007. He is currently working toward his M.S. degree in Computer Science and Engineering at the same university and holding a research assistant position in the Router Laboratory, University of Tehran. His main research interests include Intelligent Route Control, Network Protocol Design and Optimization, and Wireless Networking.

Ahmad Khonsari got his Ph.D. in Computer Science from University of Glascow, UK, in 2003. He joined the ECE Dept. of Univ. of Tehran, Tehran, Iran, as an Assistant Professor in September 2005. His research interest includes networking and distributed systems and performance modeling and evaluation.